



Published in final edited form as:

Mucosal Immunol. 2015 July ; 8(4): 896–905. doi:10.1038/mi.2014.120.

Thrombospondin-1 restrains neutrophil granule serine protease function and regulates the innate immune response during *Klebsiella pneumoniae* infection

Yani Zhao, MD PhD¹, Tolani F. Olonisakin, BS¹, Zeyu Xiong, MD¹, Mei Hulver, BS¹, Sameera Sayeed, PhD MPH¹, Min Ting Yu¹, Alyssa D. Gregory, PhD¹, Elizabeth J. Kochman, MD¹, Bill B. Chen, PhD¹, Rama K. Mallampalli, MD^{1,2}, Ming Sun, PhD³, Roy L. Silverstein, MD⁴, Donna B. Stolz, PhD³, Steve D. Shapiro, MD¹, Anuradha Ray, PhD¹, Prabir Ray, PhD¹, and Janet S. Lee, MD^{1,5}

¹Department of Medicine, Division of Pulmonary, Allergy, and Critical Care Medicine, University of Pittsburgh, Pittsburgh, PA 15213

²Medical Specialty Service Line, Veterans Affairs Pittsburgh Healthcare System, Pittsburgh PA 15240

³Department of Cell Biology and Center for Biologic Imaging, University of Pittsburgh, Pittsburgh, PA 15213

⁴Department of Medicine, Medical College of Wisconsin and Blood Research Institute, Blood Center of Wisconsin, Milwaukee, WI, 53233

⁵Vascular Medicine Institute, University of Pittsburgh, Pittsburgh, PA 15213

Abstract

Neutrophil elastase (NE) and cathepsin G (CG) contribute to intracellular microbial killing but, if left unchecked and released extracellularly, promotes tissue damage. Conversely, mechanisms that constrain neutrophil serine protease activity protect against tissue damage but may have the untoward effect of disabling the microbial killing arsenal. The host elaborates thrombospondin-1 (TSP-1), a matricellular protein released during inflammation, but its role during neutrophil activation following microbial pathogen challenge remains uncertain. Mice deficient in thrombospondin-1 (*thbs1*^{-/-}) showed enhanced lung bacterial clearance, reduced splenic dissemination, and increased survival compared with WT controls during intrapulmonary *Klebsiella pneumoniae* infection. More effective pathogen containment was associated with reduced burden of inflammation in *thbs1*^{-/-} mouse lungs compared with WT controls. Lung NE activity was increased in *thbs1*^{-/-} mice following *Klebsiella pneumoniae* challenge, and *thbs1*^{-/-} neutrophils showed enhanced intracellular microbial killing that was abrogated with recombinant TSP-1 administration or WT serum. *Thbs1*^{-/-} neutrophils exhibited enhanced NE and CG

Users may view, print, copy, and download text and data-mine the content in such documents, for the purposes of academic research, subject always to the full Conditions of use:http://www.nature.com/authors/editorial_policies/license.html#terms

Corresponding author: Janet S. Lee, M.D., 3459 Fifth Avenue, Montefiore University Hospital NW628, Pittsburgh, PA, 15213, U.S.A.; fax: 412.692-2260; leejs3@upmc.edu; tel: 412.692.2328.

Conflict of Interest: The authors declare no conflict of interest.

enzymatic activity and a peptide corresponding to amino acid residues 793–801 within the type 3 repeats domain of TSP-1 bridled neutrophil proteolytic function and microbial killing in vitro. Thus, TSP-1 restrains proteolytic action during neutrophilic inflammation elicited by *Klebsiella pneumoniae*, providing a mechanism that may regulate the microbial killing arsenal.

Keywords

thrombospondin-1; neutrophil; bacterial killing; *Klebsiella pneumoniae*

Introduction

Thrombospondin-1 (TSP-1) is a matricellular protein that exists as a trimer of identical ~150–180 kDa subunits tethered together by disulfide bonds^{1,2}. A major source of TSP-1 is platelet α -granules, with TSP-1 being released upon platelet activation^{3–5}. Thrombospondin-1 also exists in plasma at low concentrations under basal conditions, and is made by numerous cells including myeloid-derived cells such as neutrophils^{6,7}. Given its adhesive nature, TSP-1 can bind to the surface of platelets, extracellular matrix, and a number of other cells including fibroblasts, smooth muscle cells, endothelium, neutrophils and macrophages, providing a multiplicity of potential cell-cell and cell-matrix interactions². Thus, it is not surprising that TSP-1 has been implicated in a number of important biological functions such as embryogenesis, wound repair, tumor growth and metastasis, angiogenesis, hemostasis and inflammation^{2,5,8–11}.

Others have previously shown that platelet proteins such as TSP-1 are found in the airspace of patients with acute respiratory distress syndrome (ARDS) and TSP-1 concentrations correlate with composite injury scores that quantify the degree of lung injury¹². The original description of mice deficient in TSP-1 (*thbs1*^{-/-}) showed spontaneous development of non-infectious pneumonia and the predisposition to develop inflammation due to impaired homeostasis¹³. We recently demonstrated that, although *thbs1*^{-/-} mice do not spontaneously develop non-infectious pneumonia, these mice exhibit a defect in their ability to resolve from injurious stimuli to the lungs¹⁴. We have also shown that IL-10 is essential for recovery of lung inflammation during the late phase of bacterial infection^{14,15}. In an experimental model of lung injury, we further show that the bridging function of thrombospondin-1 is required for optimal triggering of macrophage IL-10 production following contact recognition of apoptotic neutrophils that is necessary for effective resolution of inflammation^{14,15}. It remains unclear, however, what the role of TSP-1 is, if any, during bacterial pneumonia, an important cause of morbidity and mortality worldwide and a well-known risk factor for ARDS¹⁶.

Neutrophils are innate immune effector cells of microbial killing and are critical for pulmonary host defense against pathogen. Two major modes of intracellular killing are operant in neutrophils: (1) oxygen-dependent mechanism involving the recruitment and activation of the NADPH oxidase complex, the generation of oxygen free radicals and superoxide, resulting in myeloperoxidase-mediated halogenation to form hypochlorous acid; (2) the release of cytosolic granule contents within the phagosome, comprised of neutrophil

serine proteases, the activation of these proteases within the phagosome¹⁷⁻¹⁹ and the contribution of anti-microbial proteins²⁰. Neutrophil elastase (NE), a key granule serine protease, degrades outer membrane protein A on the surface of gram negative bacteria²¹ and is an important contributor to the oxygen-independent arm of microbial killing. While effective neutrophil microbial killing is required to thwart collateral tissue damage and organ injury induced by microbial-host interactions, the host also requires mechanisms to curtail its microbial killing arsenal to prevent subsequent collateral tissue damage and organ injury. Indeed, unbridled neutrophil protease activity is associated with lung injury or acute respiratory distress syndrome in humans²². Thus, a fine balance is required for effective neutrophil microbial killing activity on the one hand and the curtailment of an overvigorous host inflammatory response on the other.

TSP-1 is a competitive inhibitor of serine proteases such as plasmin, preventing the cleavage of fibrinogen in vitro with stoichiometric predictions demonstrating one mole of TSP-1 interacting with one mole of plasmin²³. This prompted further studies showing that TSP-1 binds and competitively inhibits the enzymatic activity of purified neutrophil elastase (NE) and cathepsin G (CG) in vitro^{3,4}. These findings suggest a regulatory role for TSP-1 during inflammation, but how TSP-1 modulates neutrophil function during the innate immune response to bacterial pathogens is unclear.

Results

Increased bacterial clearance from the lungs, reduced splenic dissemination, and enhanced survival following intratracheal instillation of *Klebsiella pneumoniae* in mice deficient in TSP-1

To investigate the role of TSP-1 in pulmonary host defense, *thbs1*^{-/-} mice were inoculated with the bacterial pathogen *Klebsiella pneumoniae* (*K. pneumoniae*) at 4×10^3 cfu. At 48 and 72 h following intratracheal inoculation, *thbs1*^{-/-} mice showed reduced bacterial burden in the lungs compared with WT mice as measured by CFU/lung (Figure 1A). Consistent with the findings in the lungs, *thbs1*^{-/-} mice showed reduced splenic dissemination compared with WT mice (Figure 1B). Thus, pulmonary host defense is enhanced during bacterial pneumonia in the absence of TSP-1 that is associated with reduced systemic dissemination. We next determined whether the enhanced bacterial clearance in *thbs1*^{-/-} mice confers a survival advantage during bacterial pneumonia with *K. pneumoniae*. At an inoculum of 1.2×10^4 CFU, LD₅₀ was achieved at 72 h in WT mice (Figure 1C). Kaplan-Meier curve followed by log-rank test showed enhanced survival in *thbs1*^{-/-} mice compared with WT mice (p=0.02, n=20 per group). The median survival for *thbs1*^{-/-} mice was 312 h (13 days), compared with 72 h (3 days) for WT mice. A kinetics study examining responses of WT and *thbs1*^{-/-} mice 24, 48, 72, and 96 h following intratracheal inoculation (1.8×10^3 cfu) indicated that, by 72 and 96 h, *thbs1*^{-/-} mice were clearing bacteria from the lungs faster than WT mice (Supplemental Figure 1). Consistent with our prior findings²⁴, *thbs1*^{-/-} mice show deficiency in IL-10 which is required for optimal resolution of lung inflammation during the late phase after infection¹⁵. Taken together, TSP-1 deficiency improves early lung bacterial clearance, reduces systemic dissemination, and confers increased survival during bacterial pneumonia induced by *K. pneumoniae*. However, *thbs1*^{-/-} mice may later

succumb to sub-optimal resolution from injury due to inability to trigger full IL-10 responses in the lungs.

thbs1*^{-/-} mice show enhanced lung NE activity and reduced parenchymal inflammation following intratracheal *K. pneumoniae

TSP-1 can bind and induce the motility and chemotaxis of neutrophils *in vitro*²⁵⁻²⁸, and we have previously reported that *thbs1*^{-/-} mice show slightly higher leukocyte counts in the airspaces under basal conditions²⁴. Despite this, total leukocyte and neutrophil recruitment into the alveolar spaces were not different between *thbs1*^{-/-} and WT mice following intratracheal *K. pneumoniae* (Figure 2A–B). Within the lung parenchymal compartment, *thbs1*^{-/-} mice showed reduction in IL-6, IL-10, G-CSF, GM-CSF, KC, and MCP-1 but not TNF- α concentrations compared to WT controls (Figure 2C). Lung myeloperoxidase (MPO) activity, an indicator of total neutrophil content in tissue homogenates, showed no differences at 48 h (Figure 2D). By 72 h, however, *thbs1*^{-/-} lungs showed reduced MPO activity in agreement with reduced total airspace protein concentrations (Figure 2E), a marker of lung injury. Moreover, histologic examination showed lower neutrophil burden in the lungs of *thbs1*^{-/-} mice (Figure 2F, Supplemental Figure 2), and semi-quantitative morphometric analysis of lung tissue indicated significantly lower inflammation score in *thbs1*^{-/-} lungs compared to WT (Figure 2G). These findings suggest that a more effective pulmonary host defense and early containment of bacterial pathogen in *thbs1*^{-/-} mice are associated with an overall reduction in the intensity of the lung inflammatory response. We next tested the possibility whether the absence of TSP-1 may contribute to enhanced neutrophil function and provide effective containment of bacterial pathogen.

Previous reports have shown the requirement for neutrophil elastase (NE), a serine protease stored within azurophilic granules of neutrophils, for adequate bactericidal activity against gram negative bacteria such as *E. coli* and *K. pneumoniae*^{21,29}. Lung tissue homogenates of *thbs1*^{-/-} mice showed enhanced NE compared with the lungs of WT mice at 48 and 72 h following intratracheal challenge with *K. pneumoniae* (Figure 2H). Taken together, *thbs1*^{-/-} mice show increased lung NE associated with reduced intensity in the inflammatory response, suggesting the possibility that TSP-1 may regulate NE activity to restrain microbial killing with consequent alterations in the host inflammatory response.

***thbs1*^{-/-} neutrophils show enhanced microbial killing that is reversed by administration of recombinant TSP-1 or WT serum**

To more closely examine intracellular microbial killing capacity, *thbs1*^{-/-} and WT neutrophils were obtained following intraperitoneal inoculation with *K pneumoniae*. Neutrophils were washed and treated with gentamicin to remove extracellular, membrane attached bacteria. At time 0, neutrophils from *thbs1*^{-/-} and WT mice ingested similar numbers of bacteria as indicated by CFU following lysis of cells (Figure 3A). However, after 60 min incubation, *thbs1*^{-/-} neutrophil lysates showed significantly less viable bacteria compared with WT neutrophil lysates (Figure 3A), indicating enhanced microbial killing in the absence of TSP-1. The addition of recombinant TSP-1 (rTSP-1) just prior to *K. pneumoniae* challenge *in vivo* eliminated the enhanced bacterial killing function of *thbs1*^{-/-} neutrophils near to the level of WT neutrophils, suggesting a specific role of TSP-1 in

restraining neutrophil microbial killing (Figures 3B). Moreover, while WT neutrophils showed a 2.3 fold reduction in viable bacteria over time with *ex vivo* incubation, *thbs1*^{-/-} neutrophils showed a 17.8 fold reduction (mean-fold reduction in CFU/10⁶ PMN ± SEM: 2.3 ± 0.2 vs 17.8 ± 6.3, p < 0.05). Compared to *thbs1*^{-/-} neutrophils treated with vehicle alone, *thbs1*^{-/-} neutrophils pre-treated with rTSP-1 showed 5.5 fold reduction over time with *ex vivo* incubation (mean-fold reduction in CFU/10⁶ PMN ± SEM: 17.8 ± 6.3 vs 5.5 ± 0.3, p < 0.05). Thus, neutrophils show enhanced microbial killing in the absence of TSP-1 and addition of rTSP-1 can mitigate this response.

We next examined microbial killing by WT and *thbs1*^{-/-} neutrophils following *K. pneumoniae* infection *in vitro* to determine whether *in vitro* can recapitulate *in vivo* findings. At a multiplicity of infection of 50:1, *thbs1*^{-/-} neutrophils showed enhanced microbial killing compared to WT neutrophils (Figure 3C). The enhanced microbial killing observed in *thbs1*^{-/-} neutrophils could be reversed when bacteria incubated with WT serum rather than homologous serum was given to *thbs1*^{-/-} neutrophils (Figure 3D). Moreover, when bacteria incubated in *thbs1*^{-/-} serum was given to WT neutrophils, these neutrophils showed enhanced microbial killing compared with WT neutrophils that received bacteria incubated in homologous serum (Figure 3E). These experiments collectively indicate that neutrophil microbial killing is altered by TSP-1 and that the major source of TSP-1 is extracellular in origin.

***thbs1*^{-/-} neutrophils show enhanced neutrophil elastase and cathepsin G activity but normal respiratory burst and morphology**

Previous reports have shown that TSP-1 can bind and competitively inhibit purified cathepsin G and NE *in vitro*^{3,4}. However, it is unknown whether TSP-1 can constrain neutrophil proteolytic function by inhibiting granule serine protease activity. As NE is the predominant serine protease critical in non-oxidative effector killing of microbial pathogen and degrades outer membrane protein A (OmpA) on the surface of gram-negative bacteria^{18,21,29,30}, we examined the NE activity of tissue-recruited peritoneal-derived *thbs1*^{-/-} and WT neutrophils. *Thbs1*^{-/-} neutrophils showed enhanced NE activity compared with WT neutrophils, as measured by the rate of enzymatic hydrolysis of substrate N-methoxysuccinyl-Ala-Ala-Pro-Val *p*-nitroanilide (Figure 4A). While N-methoxysuccinyl-Ala-Ala-Pro-Val *p*-nitroanilide is an excellent substrate for NE but not Cathepsin G³¹, protease 3 is a neutrophil serine protease contained within azurophilic granules that can also hydrolyze N-methoxysuccinyl-Ala-Ala-Pro-Val *p*-nitroanilide³²⁻³⁴. However, neutrophils obtained from mice deficient in neutrophil elastase (*Ela2*^{-/-}) showed minimal to no measureable ability to hydrolyze N-methoxysuccinyl-Ala-Ala-Pro-Val *p*-nitroanilide, indicating that NE accounts for the serine protease activity involved in this reaction (Figure 4A).

A mixing experiment was conducted to test whether WT neutrophils possessed a factor that could inhibit the enhanced NE activity observed in *thbs1*^{-/-} neutrophils. Increasing the ratio of WT neutrophil lysates (1:3, 2:3, 3:3) added to the substrate mixture containing a fixed amount of *thbs1*^{-/-} neutrophil lysates dose-dependently reduced the NE activity to the level observed in WT neutrophils (Figure 4B). Thus, neutrophils derived from an *in vivo*

environment that lacks TSP-1 show unrestrained NE activity and reconstitution with lysates from neutrophils derived from mice with intact TSP-1 eliminated this effect. Suc-Ala-Ala-Pro-Phe-p-nitroanilide is a chemical substrate for cathepsin G but not NE³¹, and *thbs1*^{-/-} neutrophils also showed enhanced cathepsin G activity compared with WT neutrophils (Figure 4C). Taken together, the data indicate TSP-1 regulates both NE and cathepsin G activity in neutrophils.

To determine whether TSP-1 alters neutrophil respiratory burst, we measured the oxidation of dihydro-rhodamine to rhodamine in *thbs1*^{-/-} and WT neutrophils, a clinically relevant test performed on patient neutrophils suspected of NADPH oxidase dysfunction. *thbs1*^{-/-} neutrophils showed similar respiratory burst to WT neutrophils (Figure 4D), indicating that reactive oxygen species generation is not exaggerated in *thbs1*^{-/-} neutrophils that may account for the altered pulmonary host defense. We also compared the ultrastructure of *thbs1*^{-/-} neutrophils with WT neutrophils, and show similar morphology (Figure 4E). Furthermore, *thbs1*^{-/-} neutrophils show similar in vitro phagocytosis of fluorescently-labeled *E. coli* bioparticles compared to WT neutrophils (Figure 4F). Collectively, these findings suggest that TSP-1 impacts neutrophil proteolytic function by restraining NE and cathepsin G activity but do not significantly alter the respiratory burst, phagocytosis, or morphology.

Peptides generated from the thrombospondin-1 type III repeats domain inhibit protease activity of neutrophils

The type III repeats domain is a region within TSP-1 that harbors possible inhibitory reactive centers bearing striking similarity to consensus sequences derived from the Kazal and Streptomyces subtilisin inhibitor family members^{35,36}. We generated peptides corresponding to residues 734–742 (DP-9 peptide) and 793–801 (DV-9 peptide), two stretches of eight amino acids within the Type III repeats domain, bearing reactive-site sequence similarity to select members of the Kazal family of subtilisin inhibitors. Moreover, a peptide corresponding to amino acid residues 734–742 previously showed the ability to inhibit activity of purified cathepsin G in vitro, whereas a peptide corresponding to residues 793–801 showed inhibitory activity to both purified cathepsin G and NE³⁵. We generated a third peptide corresponding to residues 854–862 (DA-9) without reactive-site sequence similarity or known inhibitory activity³⁵ that was used as control. Unlike in vitro conditions involving purified enzyme and inhibitor of known concentrations, activated neutrophils isolated from thioglycollate-stimulated peritoneum possess numerous proteases and enzymes that can reduce peptide efficacy. Thus, peptides were utilized in excess concentration to determine whether discrete regions of the type III repeat domain exhibit inhibitory NE and CG activity by a mechanism of substrate competition. Lysates prepared from WT neutrophils were tested for NE activity, as measured by the rate of enzymatic hydrolysis of substrate N-methoxysuccinyl-Ala-Ala-Pro-Val *p*-nitroanilide, in the presence or absence of peptides DV-9, DP-9, and control peptide DA-9.

Neutrophil elastase activity was dose-dependently inhibited in the presence of DV-9. DV-9 reduced NE activity by 28% at 1.25 mM and 89% at 2.5 mM peptide, whereas DP-9 (or DA-9 showed no effect (Figure 5A). Cathepsin G activity, on the other hand, as measured

by the rate of enzymatic hydrolysis of substrate N-Suc-Ala-Ala-Pro-Phe p-nitroanilide, was dose-dependently inhibited by DV-9 by 54% at 1.25 mM, and 86% at 2.5 mM (Figure 5B). DP-9 at the higher concentration of 2.5 mM inhibited CG activity by 20%, whereas DA-9 showed no effect (Figure 5B). Thus, residues 793–801 within the break sequence of the calcium binding loops located in the type 3 repeats domain of TSP-1 can restrain neutrophil proteolytic function by effectively inhibiting NE and CG enzymatic activity. Residues 734–742 of TSP-1 showed a weak inhibitory effect on CG enzymatic activity within neutrophils.

Peptides corresponding to residues 793–801 of the type III repeats domain impair neutrophil microbial killing of *K. pneumoniae*

We next tested whether administration of peptide DV-9, showing inhibitory activity against NE and CG proteolytic function contained within neutrophil lysates, can alter neutrophil microbial killing. Neutrophils harvested from mice administered DV-9 peptide showed significantly higher viable bacteria at 30 and 90 minutes post-bacterial inoculation than neutrophils from vehicle-treated mice (Figure 6). Neutrophils from vehicle-treated mice showed 8.3 fold reduction in viable bacteria with ex vivo incubation over time, whereas neutrophils from peptide DV-9 treated mice showed 3.5 fold reduction in viable bacteria over time (mean-fold reduction in CFU/10⁶ PMN ± SE: 8.3 ± 2.0 vs 3.5 ± 0.6, $p < 0.05$). Thus, the administration of a peptide corresponding to the type III repeats region of TSP-1 can impair neutrophil microbial killing machinery against *K. pneumoniae*.

Discussion

Mice deficient in TSP-1 show enhanced bacterial clearance from the lungs induced by *K. pneumoniae*, reduced splenic dissemination, and increased survival compared with WT controls. Lungs of *thbs1*^{-/-} mice show enhanced NE activity but reduced parenchymal inflammation and injury, suggesting that early containment of bacterial pathogen and microbial killing reduces overall intensity of the inflammatory response following intratracheal challenge with *K. pneumoniae*. In the complete absence of TSP-1, neutrophil serine protease NE and cathepsin G activity are intensified as is intracellular microbial killing in a model dependent upon an effective host response to live bacterial pathogen. We suggest that TSP-1 provides an endogenous mechanism to curtail neutrophil proteolytic function during inflammation and identify a region within the break sequence of the calcium binding loops located in the type 3 repeats domain of TSP-1 that may be involved in this interaction.

We have recently shown that mice deficient in TSP-1 are prone to experimental LPS-induced lung injury¹⁴, a well-known non-infectious inducer of inflammation and injury causing vascular leak. However, with live bacterial pathogen, *thbs1*^{-/-} mice show more effective containment of bacteria and reduced lung inflammation and injury. Susceptibility to sterile injury but enhanced ability to combat microbial challenge is a phenotype that is consistent with unbridled neutrophil protease activity. Others have shown improved host defense in *thbs1*^{-/-} mice against live bacterial or fungal challenge^{37,38}, but the mechanisms for these observations were not well understood. *thbs1*^{-/-} mice showed improved survival in a cecal ligation puncture model of sepsis involving polymicrobial infection in addition to

an intra-peritoneal challenge with live *E. coli* bacteria³⁷. In an experimental model of systemic candidiasis, *thbs1*^{-/-} mice also showed less dissemination of *Candida albicans* systemically and improved survival³⁸. While both studies suggested that TSP-1 impairs phagocytic capacity as a potential mechanism for survival differences following pathogen challenge, it remains unclear how TSP-1 would mediate the defect in phagocytosis. In contrast, we have previously reported WT and *thbs1*^{-/-} alveolar macrophages show similar ability to phagocytize apoptotic neutrophils in vivo¹⁴, and herein, show no significant differences between WT and *thbs1*^{-/-} neutrophils to phagocytize fluorescently-labeled *Escherichia coli* (*E. coli*) bioparticles in vitro. Similar to our findings, however, *thbs1*^{-/-} mice showed reduced fungal burden and reduced host inflammatory response in the kidneys in the *Candida albicans* (*C. albicans*) model³⁸, inviting speculation that effective containment of pathogen in *thbs1*^{-/-} mice also reduced the burden of inflammation following systemic *C. albicans* challenge. Indeed, enhanced neutrophil intracellular microbial killing in *thbs1*^{-/-} mice due to unopposed serine protease activity could potentially provide an explanation for the findings in the prior studies.

Non-oxygen dependent neutrophil microbial killing mechanisms are a critical component of host defense. Mice deficient in neutrophil elastase (*Ela2*^{-/-}) show impaired host defense and survival in gram negative bacterial sepsis from intraperitoneal *K. pneumoniae* or *E. coli* infection²⁹, systemic candidiasis from *C. albicans*¹⁸, and pneumonia from *Pseudomonas aeruginosa* (*P. aeruginosa*)³⁹. Mice deficient in cathepsin G (*CtsG*^{-/-}) show impaired survival following *Staphylococcus aureus*¹⁸, and *Streptococcus pneumoniae* (*S. pneumoniae*)⁴⁰ infection. Thus, it is not surprising that neutrophil elastase and cathepsin G double knockout mice (*Ela2*^{-/-}*CtsG*^{-/-}) show increased susceptibility to fungal infection from *Aspergillus fumigatus* despite normal neutrophil recruitment and phagocytic activity³⁰ and essentially worse survival than *CtsG*^{-/-} mice from *S. pneumoniae* pneumonia with greater degree of lung injury from failure to effectively contain pathogen-derived virulence factors⁴⁰.

Surprisingly, mice deficient in SERPINB1 (*serpinb1*^{-/-}), a serine protease inhibitor of NE, cathepsin G and proteinase 3, fail to clear *P. aeruginosa* pneumonia, show worse survival and inflammation⁴¹. Although SERPINB1 is expressed in the cytoplasm of neutrophils, the data would indicate that SERPINB1 mainly functions to protect against the tissue injurious effects of extracellular neutrophil serine proteases and the degradation of host defense molecules such as surfactant protein D^{41,42}. Interestingly, *Ela2*^{-/-}*CtsG*^{-/-} mice are resistant to endotoxic shock, and are protected from vascular leak and lung injury³⁰, supporting the notion that unmitigated release of neutrophil serine proteases into the extracellular space can lead to fulminant tissue injury. Thus, the phenotype of *thbs1*^{-/-} mice appears to be the reverse of *Ela2*^{-/-}*CtsG*^{-/-} mice. Given TSP-1 effects on neutrophil microbial killing and intracellular protease activity, our data indicates that TSP-1 may be involved in the early regulation and compartmentalization of neutrophil granule serine proteases.

TSP-1 is a matricellular protein with numerous ligands and potential binding partners in vitro¹¹. In kinetic studies examining TSP-1 inhibition of NE substrate hydrolysis, 1 mol of TSP-1 trimer binds to 2.7 ± 0.3 mol of NE with a site binding constant of 57 ± 13 nM⁴. In assessing TSP-1 inhibition of cathepsin G substrate hydrolysis, 1 mol of TSP-1 trimer binds

to 2.9 ± 0.4 mol of cathepsin G with a site binding constant of 7.0 ± 3.5 nM³. These site binding constants were obtained in the presence of calcium, as TSP-1 interactions with NE and cathepsin G are sensitive to calcium-dependent conformational changes within the type III repeats domain of TSP-1^{3,4}. In the absence of calcium, the reversible inhibition of NE and CG by TSP-1 is enhanced^{3,4}. Given the complex nature of TSP-1 binding, predictions of physiological interactions remains challenging, and highlights the importance of clarifying the role of TSP-1 in the context of cell-based and in vivo studies. Various reports in vitro suggest TSP-1, either released in solution or adhered to a variety of ligands or binding partners, bind and induce motility of neutrophils, conceivably directing their migration in tissue^{25–28,43}. We found no evidence that TSP-1 significantly contributes to neutrophil recruitment in our model. Although activated rabbit and human neutrophils produce TSP-1⁶, our findings indicate that the major contributor of TSP-1 is extracellular in origin, likely released in solution during inflammation and adhering to neutrophils to modulate their activity.

In conclusion, we have identified a novel role for TSP-1 in regulating neutrophil function during the innate immune response to *K. pneumoniae* infection. Our findings suggest that TSP-1 can bridle neutrophil proteolytic activity and microbial killing through the inhibitory action of its type III repeat domain, providing one mechanism by which TSP-1 regulates the innate immune response. Although the host has evolved mechanisms to curtail the extracellular tissue-damaging effects of NSPs, thrombospondin-1 appears to curb neutrophil proteolytic function with unintended consequences for host defense. Some chronic inflammatory lung diseases that demonstrate protease/anti-protease imbalance paradoxically show impaired ability to effectively kill colonizing bacteria despite large numbers of neutrophils. Free neutrophil elastase activity in the BAL fluid of children with cystic fibrosis early in life is a strong independent risk factor for the development of bronchiectasis⁴⁴, and inability to control infection precedes, initiates, and sustains inflammation in CF airways⁴⁵. Neutrophils from cystic fibrosis patients show increase in TSP-1 gene expression by microarray compared to neutrophils from control healthy subjects⁴⁶. Moreover, cystic fibrosis patients show increased circulating activated platelets with formation of heterotypic aggregates and surface P-selectin expression^{47,48}, inviting speculation that excessive TSP-1 release in some inflammatory lung diseases may contribute to neutrophil dysfunction and impaired ability to effectively kill colonizing microbes.

Material and methods

Animals

Animal studies were conducted in accordance with the recommendations in the Guide for the Care and Use of Laboratory Animals of the National Institutes of Health. The animal protocol was approved by the Institutional Animal Care and Use Committee at the University of Pittsburgh. C57BL/6J (#000664) and *thbs1*^{-/-} (B6.129S2-*Thbs1*^{tm1Hyn/J}, #006141) mice were obtained from the Jackson Laboratory (Bar Harbor, ME). *Thbs1*^{-/-} mice were backcrossed to C57Bl/6 mice 9 times and a colony was subsequently established at the University of Pittsburgh. *Ela2*^{-/-} (B6.129X1-*Ela2*^{tm1Sds/J}) mice were obtained from a colony at the University of Pittsburgh. All experimental procedures were performed in age

(8–12 week old) and gender-matched mice. The animals were housed and maintained in a pathogen-free environment.

Experimental Bacterial Pneumonia model

Klebsiella pneumoniae strain 43816, serotype 2 (American Type Culture Collection, Manassas, VA) was grown in tryptic soy broth overnight at 37 °C. 1 mL of this overnight culture was inoculated into fresh tryptic soy broth and grown for 2 hours. A standard curve of absorbance (OD₆₀₀) was generated to determine mid-log phase of growth and inoculum concentrations. Inoculum concentration, measured in colony forming units (CFU), was determined by serial 10-fold dilutions of bacteria plated on tryptic soy agar plates (Sigma, St. Louis, MO). Bacteria was harvested, washed and resuspended in PBS before use. WT and *thbs1*^{-/-} mice were anesthetized with isoflurane and 10³ CFU of *K. pneumoniae* in a total volume of 100 µL was carefully administered intratracheally under direct visualization using a sterile 200 µL pipet with filtered tip positioned just above the vocal cords. For mortality studies, 10⁴ inoculum was utilized. The inoculums were confirmed by plating serial 10-fold dilutions on tryptic soy broth agar plates.

Bronchoalveolar Lavage fluid collection

Animals were euthanized at pre-determined time points with isoflurane inhaled anesthetic overdose within a closed container system followed by cardiac puncture and exsanguination. Methods for obtaining bronchoalveolar lavage (BAL) total cell counts and differential and lung histology have been previously reported²⁴.

Measurements of lung and spleen bacterial burden

The left lung and spleen were removed following euthanasia at specified time points. For enumerating bacterial CFUs in the lungs and spleens, tissue was homogenized in 1 mL of sterile diH₂O. 100 µl homogenates were plated by 10-fold serial dilution on tryptic soy agar plates. Bacterial CFU was counted after an overnight incubation at 37 °C.

Measurement of lung cytokines and chemokines

Total protein in lung tissue homogenates were quantified using the Pierce BCA Protein Assay Kit (Thermo Scientific, Rockford, IL). The volume of lung tissue homogenate corresponding to 100 µg total protein from each sample was used to perform ELISA. ELISA duoset antibodies for measuring TNF-α, IL-6, IL-10, G-CSF, GM-CSF, KC, MCP-1 were obtained from R&D Systems (Minneapolis, MN).

MPO assay

Lung tissue homogenates in 0.5% hexadecyl-trimethylammonium bromide (HTAB) buffer (5g of HTAB in 1 liter of MPO buffer, where MPO buffer contains 6.8g of KH₂PO₄ and 8.7g of K₂HPO₄ in 1 liter of water) were sonicated for 30 s and then centrifuged at 20,000 g for 4 minutes. 7 µl of supernatant was transferred into a 96-well plate, 200 µl of *O*-dianisidine hydrochloride solution is added immediately prior to reading the optical density at 450 nm at 1 min and 10 minutes. The MPO activity was calculated by using the following

formula as previously described⁴⁹: units of MPO activity in each well = (the change in absorbance [between 0 and 60S]/time [min]) $\times 1.13 \times 10^{-2}$.

Neutrophil serine protease activity measurements

Neutrophil elastase activity in lung tissue homogenates was measured utilizing a previously described method⁵⁰. Briefly, 1 mg lung tissue homogenates were incubated with 0.1 mol/L Tris-HCl buffer (pH 8.0) containing 0.5 mol/L NaCl and 1 mmol/L N-methoxysuccinyl-Ala-Ala-Pro-Val *p*-nitroanilide (Sigma, St. Louis, MO) at 37 °C for 24 hours. The degradation of substrate in samples was measured by spectrophotometry at 405 nm. To measure serine protease activity within neutrophils, neutrophils were harvested from the peritoneum at 6 hours following intra-peritoneal injection with 2 ml of 3% thioglycollate. Cell counts were performed manually using a hemocytometer. Cytospins confirmed >90% neutrophils at 6 h harvest. 1×10^6 neutrophils per well were seeded into a 24-well plate. Non-adherent cells were gently washed off after a 30 min incubation. Remaining adherent cells were lysed with lysis buffer containing leupeptin (Cell Signaling Technology Inc, Danvers, MA). 10 μ g total protein of lysates from each sample was incubated with 0.1 mol/L Tris-HCl buffer (pH 8.0) containing 0.5 mol/L NaCl and 1 mmol/L of NE substrate N-methoxysuccinyl-Ala-Ala-Pro-Val *p*-nitroanilide (Sigma, St. Louis, MO) or cathepsin G substrate N- Suc-Ala-Ala-Pro-Phe-*p*-nitroanilide at 37 °C for 1 hour utilizing a modified protocol from Niemann, et al⁵¹. Peptides DP-9 (Ac-DNCPFHYNP-NH₂), DV-9 (Ac-DNCQYVYNV-NH₂), and DA-9 (Ac-DNCPYVPNA -NH₂), corresponding to amino acid residues 734–742, 793–801, and 854–862 of human thrombospondin-1, respectively were generated and used in select experiments (Chi Scientific, Maynard, MA). Neutrophil lysates were incubated with 0, 1.25 mM or 2.5 mM peptides for 30 minutes before NE and cathepsin G substrates were added. The reaction was measured by spectrophotometry at 405nm over time.

Statistics

Results are reported as the mean plus or minus standard error of the mean (SEM). A Student's two-tailed *t*-test was used to compare two groups and ANOVA with Bonferroni multiple comparisons test was used for experiments involving more than one comparison. For data that was not normally distributed, Mann-Whitney rank sum test was used to compare two groups and Kruskal-Wallis test followed by a Dunn's Multiple Comparisons test was conducted for experiments involving more than one comparison. Log-rank test was performed to generate the Kaplan Meier survival curve. A *p*-value less than 0.05 was considered significant using GraphPad Prism software version 5.0 (La Jolla, CA).

Methods for the transmission electron microscopy, phagocytosis assay, microbial killing assay, and lung histology inflammation scoring are detailed in the online supplemental materials section at <http://www.nature.com/mi>

Supplementary Material

Refer to Web version on PubMed Central for supplementary material.

Acknowledgements

Funding sources include R01 HL086884 (JSL), Flight Attendant Medical Research Institute (JSL), Pilot Project Program in Hemostasis and Vascular Biology through UL1 RR024153 and UL1 TR000005 (University of Pittsburgh CTSI), the Vascular Medicine Institute, the Hemophilia Center of Western Pennsylvania, Institute for Transfusion Medicine (JSL), P01 HL114453 (RKM, PR), and a Merit Review Award from the US Department of Veterans Affairs (RKM).

References

1. Frazier WA. Thrombospondin: a modular adhesive glycoprotein of platelets and nucleated cells. *The Journal of cell biology*. 1987; 105:625–632. [PubMed: 3305519]
2. Bornstein P. Diversity of function is inherent in matricellular proteins: an appraisal of thrombospondin 1. *The Journal of cell biology*. 1995; 130:503–506. [PubMed: 7542656]
3. Hogg PJ, Owensby DA, Chesterman CN. Thrombospondin 1 is a tight-binding competitive inhibitor of neutrophil cathepsin G. Determination of the kinetic mechanism of inhibition and localization of cathepsin G binding to the thrombospondin 1 type 3 repeats. *J Biol Chem*. 1993; 268:21811–21818. [PubMed: 8408036]
4. Hogg PJ, Owensby DA, Mosher DF, Misenheimer TM, Chesterman CN. Thrombospondin is a tight-binding competitive inhibitor of neutrophil elastase. *J Biol Chem*. 1993; 268:7139–7146. [PubMed: 8463250]
5. Lawler J. The structural and functional properties of thrombospondin. *Blood*. 1986; 67:1197–1209. [PubMed: 3516249]
6. Kreis C, La Fleur M, Menard C, Paquin R, Beaulieu AD. Thrombospondin and fibronectin are synthesized by neutrophils in human inflammatory joint disease and in a rabbit model of in vivo neutrophil activation. *J Immunol*. 1989; 143:1961–1968. [PubMed: 2778318]
7. Catena R, et al. Bone marrow-derived Gr1+ cells can generate a metastasis-resistant microenvironment via induced secretion of thrombospondin-1. *Cancer discovery*. 2013; 3:578–589. [PubMed: 23633432]
8. Iruela-Arispe ML, Bornstein P, Sage H. Thrombospondin exerts an antiangiogenic effect on cord formation by endothelial cells in vitro. *Proc Natl Acad Sci U S A*. 1991; 88:5026–5030. [PubMed: 1711216]
9. Sweetwyne MT, Murphy-Ullrich JE. Thrombospondin1 in tissue repair and fibrosis: TGF- beta-dependent and independent mechanisms. *Matrix Biol*. 2012; 31:178–186. [PubMed: 22266026]
10. Lawler PR, Lawler J. Molecular basis for the regulation of angiogenesis by thrombospondin-1 and -2. *Cold Spring Harbor perspectives in medicine*. 2012; 2:a006627. [PubMed: 22553494]
11. Resovi A, Pinessi D, Chiorino G, Tarabozetti G. Current understanding of the thrombospondin-1 interactome. *Matrix Biol*. 2014
12. Idell S, et al. Platelet-specific alpha-granule proteins and thrombospondin in bronchoalveolar lavage in the adult respiratory distress syndrome. *Chest*. 1989; 96:1125–1132. [PubMed: 2530064]
13. Lawler J, et al. Thrombospondin-1 is required for normal murine pulmonary homeostasis and its absence causes pneumonia. *J Clin Invest*. 1998; 101:982–992. [PubMed: 9486968]
14. Zhao Y, et al. Thrombospondin-1 triggers macrophage IL-10 production and promotes resolution of experimental lung injury. *Mucosal Immunol*. 2013
15. Poe SL, et al. STAT1-regulated lung MDSC-like cells produce IL-10 and efferocytose apoptotic neutrophils with relevance in resolution of bacterial pneumonia. *Mucosal Immunol*. 2013; 6:189–199. [PubMed: 22785228]
16. Ranieri VM, et al. Acute respiratory distress syndrome: the Berlin Definition. *JAMA : the journal of the American Medical Association*. 2012; 307:2526–2533. [PubMed: 22797452]
17. Klebanoff SJ. Iodination of bacteria: a bactericidal mechanism. *J Exp Med*. 1967; 126:1063–1078. [PubMed: 4964565]
18. Reeves EP, et al. Killing activity of neutrophils is mediated through activation of proteases by K+ flux. *Nature*. 2002; 416:291–297. [PubMed: 11907569]

19. Segal AW. How neutrophils kill microbes. *Annu Rev Immunol.* 2005; 23:197–223. [PubMed: 15771570]
20. Ledford JG, Kovarova M, Koller BH. Impaired host defense in mice lacking ONZIN. *J Immunol.* 2007; 178:5132–5143. [PubMed: 17404296]
21. Belaouaj A, Kim KS, Shapiro SD. Degradation of outer membrane protein A in *Escherichia coli* killing by neutrophil elastase. *Science.* 2000; 289:1185–1188. [PubMed: 10947984]
22. Lee CT, et al. Elastolytic activity in pulmonary lavage fluid from patients with adult respiratory-distress syndrome. *N Engl J Med.* 1981; 304:192–196. [PubMed: 6969364]
23. Hogg PJ, Stenflo J, Mosher DF. Thrombospondin is a slow tight-binding inhibitor of plasmin. *Biochemistry.* 1992; 31:265–269. [PubMed: 1531022]
24. Zhao Y, et al. Thrombospondin-1 triggers macrophage IL-10 production and promotes resolution of experimental lung injury. *Mucosal Immunol.* 2014; 7:440–448. [PubMed: 24045574]
25. Suchard SJ, Burton MJ, Dixit VM, Boxer LA. Human neutrophil adherence to thrombospondin occurs through a CD11/CD18-independent mechanism. *J Immunol.* 1991; 146:3945–3952. [PubMed: 1674522]
26. Mansfield PJ, Boxer LA, Suchard SJ. Thrombospondin stimulates motility of human neutrophils. *The Journal of cell biology.* 1990; 111:3077–3086. [PubMed: 2269666]
27. Mansfield PJ, Suchard SJ. Thrombospondin promotes both chemotaxis and haptotaxis in neutrophil-like HL-60 cells. *J Immunol.* 1993; 150:1959–1970. [PubMed: 8436828]
28. Suchard SJ, Boxer LA, Dixit VM. Activation of human neutrophils increases thrombospondin receptor expression. *J Immunol.* 1991; 147:651–659. [PubMed: 1712815]
29. Belaouaj A, et al. Mice lacking neutrophil elastase reveal impaired host defense against gram negative bacterial sepsis. *Nat Med.* 1998; 4:615–618. [PubMed: 9585238]
30. Tkalcevic J, et al. Impaired immunity and enhanced resistance to endotoxin in the absence of neutrophil elastase and cathepsin G. *Immunity.* 2000; 12:201–210. [PubMed: 10714686]
31. Nakajima K, Powers JC, Ashe BM, Zimmerman M. Mapping the extended substrate binding site of cathepsin G and human leukocyte elastase. Studies with peptide substrates related to the alpha 1-protease inhibitor reactive site. *J Biol Chem.* 1979; 254:4027–4032. [PubMed: 312290]
32. Korkmaz B, Horwitz MS, Jenne DE, Gauthier F. Neutrophil elastase, proteinase 3, and cathepsin G as therapeutic targets in human diseases. *Pharmacol Rev.* 2010; 62:726–759. [PubMed: 21079042]
33. Kam CM, et al. Substrate and inhibitor studies on proteinase 3. *FEBS letters.* 1992; 297:119–123. [PubMed: 1551417]
34. Rao NV, et al. Characterization of proteinase-3 (PR-3), a neutrophil serine proteinase. Structural and functional properties. *J Biol Chem.* 1991; 266:9540–9548. [PubMed: 2033050]
35. Hogg PJ, Jimenez BM, Chesterman CN. Identification of possible inhibitory reactive centers in thrombospondin 1 that may bind cathepsin G and neutrophil elastase. *Biochemistry.* 1994; 33:6531–6537. [PubMed: 8204588]
36. Lu SM, et al. Predicting the reactivity of proteins from their sequence alone: Kazal family of protein inhibitors of serine proteinases. *Proc Natl Acad Sci U S A.* 2001; 98:1410–1415. [PubMed: 11171964]
37. McMaken S, et al. Thrombospondin-1 contributes to mortality in murine sepsis through effects on innate immunity. *PLoS One.* 2011; 6:e19654. [PubMed: 21573017]
38. Martin-Manso G, et al. Endogenous thrombospondin-1 regulates leukocyte recruitment and activation and accelerates death from systemic candidiasis. *PLoS One.* 2012; 7:e48775. [PubMed: 23144964]
39. Hirche TO, et al. Neutrophil elastase mediates innate host protection against *Pseudomonas aeruginosa*. *J Immunol.* 2008; 181:4945–4954. [PubMed: 18802098]
40. Hahn I, et al. Cathepsin G and neutrophil elastase play critical and nonredundant roles in lung-protective immunity against *Streptococcus pneumoniae* in mice. *Infect Immun.* 2011; 79:4893–4901. [PubMed: 21911460]
41. Benarafa C, Priebe GP, Remold-O'Donnell E. The neutrophil serine protease inhibitor serpinb1 preserves lung defense functions in *Pseudomonas aeruginosa* infection. *J Exp Med.* 2007; 204:1901–1909. [PubMed: 17664292]

42. Wright JR. Immunoregulatory functions of surfactant proteins. *Nat Rev Immunol.* 2005; 5:58–68. [PubMed: 15630429]
43. Majluf-Cruz A, et al. Residues F16-G33 and A784-N823 within platelet thrombospondin-1 play a major role in binding human neutrophils: evaluation by two novel binding assays. *J Lab Clin Med.* 2000; 136:292–302. [PubMed: 11039850]
44. Sly PD, et al. Risk factors for bronchiectasis in children with cystic fibrosis. *N Engl J Med.* 2013; 368:1963–1970. [PubMed: 23692169]
45. Armstrong DS, et al. Lower airway inflammation in infants with cystic fibrosis detected by newborn screening. *Pediatric pulmonology.* 2005; 40:500–510. [PubMed: 16208679]
46. Adib-Conquy M, et al. Neutrophils in cystic fibrosis display a distinct gene expression pattern. *Mol Med.* 2008; 14:36–44. [PubMed: 18026571]
47. O'Sullivan BP, Michelson AD. The inflammatory role of platelets in cystic fibrosis. *Am J Respir Crit Care Med.* 2006; 173:483–490. [PubMed: 16339920]
48. O'Sullivan BP, et al. Platelet activation in cystic fibrosis. *Blood.* 2005; 105:4635–4641. [PubMed: 15705796]
49. Jeyaseelan S, Chu HW, Young SK, Worthen GS. Transcriptional profiling of lipopolysaccharide-induced acute lung injury. *Infect Immun.* 2004; 72:7247–7256. doi:72/12/7247 [pii] 10.1128/IAI.72.12.7247-7256.2004. [PubMed: 15557650]
50. Ishii T, et al. Neutrophil elastase contributes to acute lung injury induced by bilateral nephrectomy. *The American journal of pathology.* 2010; 177:1665–1673. [PubMed: 20709801]
51. Niemann CU, et al. Neutrophil elastase depends on serglycin proteoglycan for localization in granules. *Blood.* 2007; 109:4478–4486. [PubMed: 17272511]

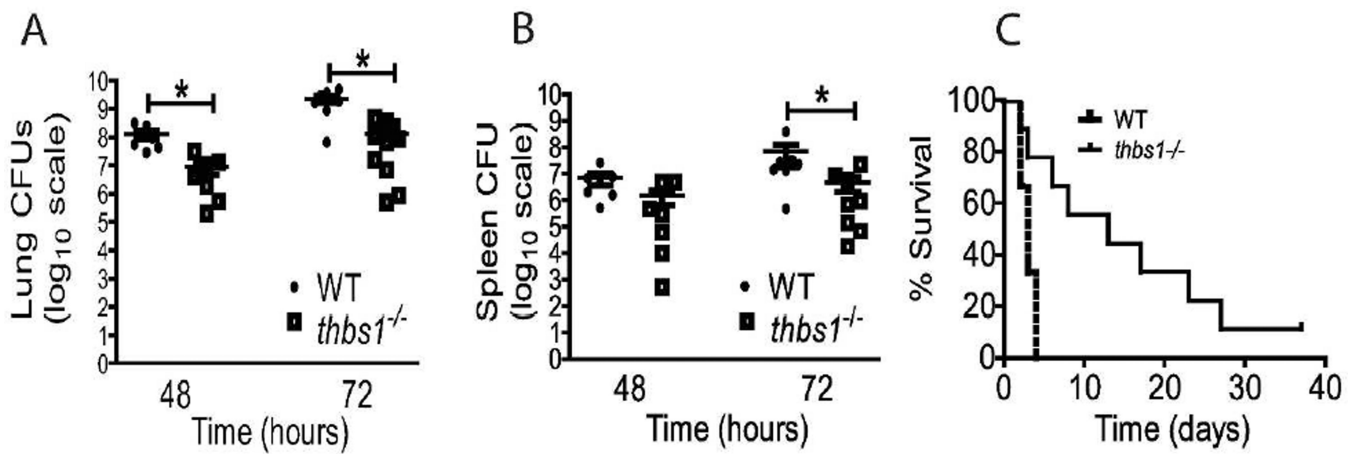


Figure 1. *thbs1*^{-/-} mice show enhanced lung bacterial clearance, reduced splenic dissemination, and enhanced survival following intratracheal *K. pneumoniae* inoculation

Colony forming units (CFU) obtained from (A) lung tissue homogenate and (B) splenic homogenate cultures of WT and *thbs1*^{-/-} mice 48 and 72 hours after i.t. inoculation with *K. pneumoniae*, n=7–10 mice/group. Kruskal-Wallis test with Dunn's multiple comparisons, *p<0.05. (C) A Kaplan-Meier survival curve of WT and *thbs1*^{-/-} mice following i.t. infection with *K. pneumoniae* (n=20 mice/genotype, p=0.02). The median survival for WT mice was 72 h (3 days) and 312 h (13 days) for *thbs1*^{-/-} mice.

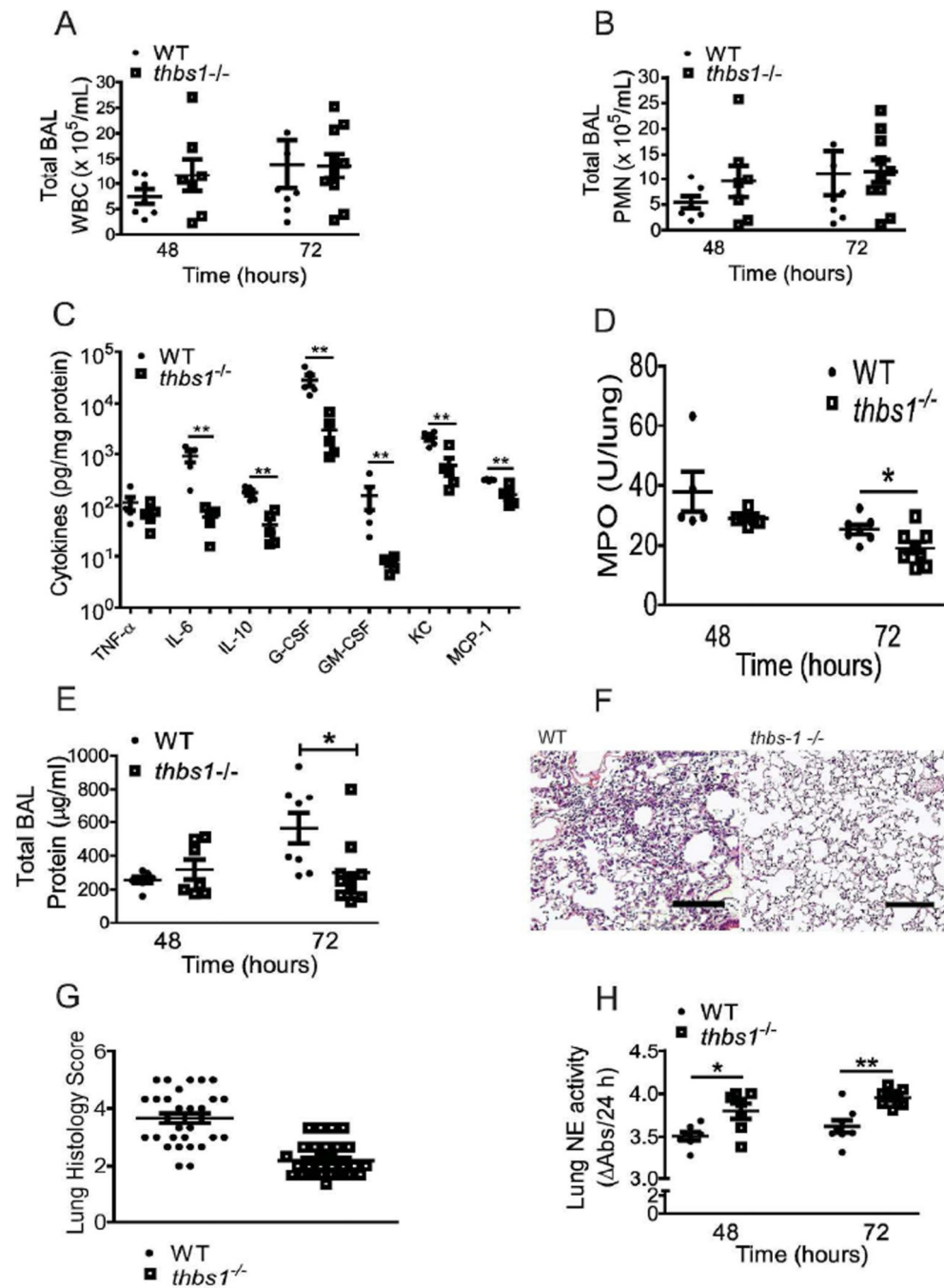


Figure 2. Reduced inflammatory response in the lung parenchyma of *thbs1*^{-/-} mice is associated with enhanced NE activity following bacterial pneumonia with *K. pneumoniae*

(A) Total BAL leukocyte counts and (B) Total BAL PMN counts obtained from WT and *thbs1*^{-/-} mice 48 and 72 hours following i.t. inoculation with *K. pneumoniae*. (C) Lung cytokine measurements in pg/mL from 100 μg protein of tissue homogenates obtained from the left lung of mice 48 hours following i.t. *K. pneumoniae*. Cytokines were measured individually by ELISA, and data is presented in one graph for simplicity. (D) MPO activity in left lung tissue homogenates measured as U/lung from WT and *thbs1*^{-/-} mice 48 and 72

hours after i.t. inoculation with *K. pneumoniae*. (E) Total BAL protein concentrations in $\mu\text{g/mL}$ from WT and *thbs1*^{-/-} mice 48 and 72 hours after i.t. inoculation with *K. pneumoniae*. (F) Representative H&E sections of R lung tissue obtained from WT and *thbs1*^{-/-} mice at 72 hours post-*K. pneumoniae* instillation. Experimental mice underwent bronchoalveolar lavage of the lung prior to tissue fixation. Scale bar = 100 μm . (G) Lung histology shows higher inflammation score in WT compared to *thbs1*^{-/-} mouse lung tissue sections from 72 h post-*K. pneumoniae* instillation, n=60 random high powered images from 3 sections/group scored by 3 blinded reviewers. The averaged score for each image is shown as individual point. (H) NE activity measured in lung tissue homogenates at 48 and 72 hours following i.t. *K. pneumoniae*. (A-E, H) n=7-10 mice/group, Mann-Whitney U rank sum test, ***p<0.0001, **p <0.01, *p<0.05.

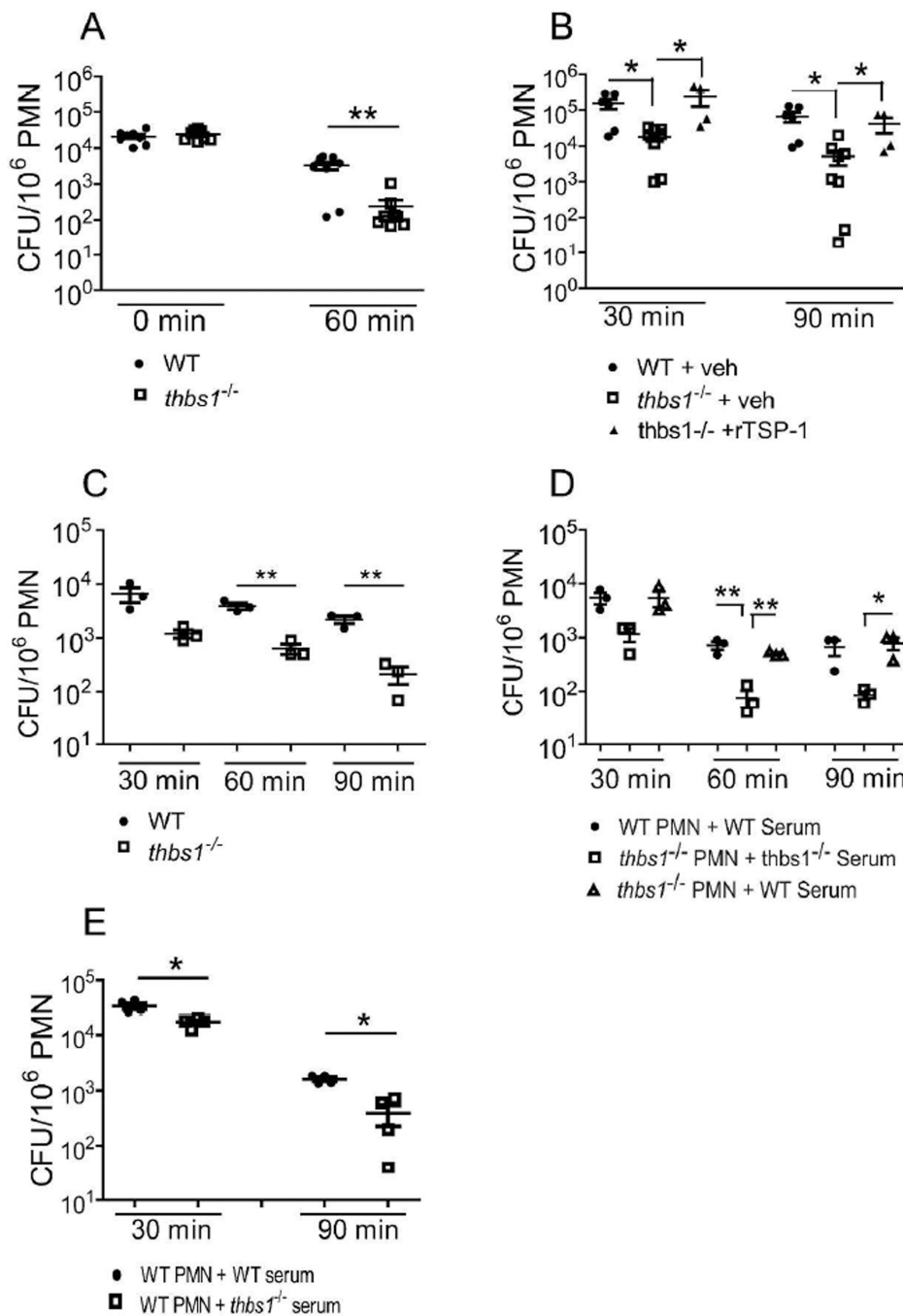


Figure 3. *thbs1*^{-/-} neutrophils show enhanced intracellular microbial killing that is reversed by administration of recombinant TSP-1 or WT serum

(A) Intracellular killing by neutrophils from WT and *thbs1*^{-/-} mice exposed to *K. pneumoniae* intraperitoneally. Neutrophils were immediately harvested and subsequently plated to quantify CFU or incubated further ex vivo for an additional 60 min prior to plating. CFU/10⁶ PMN was obtained for each sample. Data points indicate 8 samples/group using harvested neutrophils from 4 *thbs1*^{-/-} and 4 WT mice. (B) Mice were pre-treated with recombinant TSP-1 (10 μg/mouse) or PBS vehicle 30 min prior to intraperitoneal instillation

of *K. pneumoniae*. Neutrophils were harvested and subsequently plated to quantify CFU at 30 min or incubated further ex vivo for an additional 60 min prior to plating. CFU/10⁶ PMN was obtained for each sample. Data points indicate 4–8 samples/group using harvested neutrophils from 6 *thbs1*^{-/-} and 3 WT mice. (C) *In vitro* microbial killing assay with WT and *thbs1*^{-/-} neutrophils. Neutrophils were harvested from the peritoneum 6 h following 3% thioglycollate as detailed in the methods. *K. pneumoniae* was opsonized with 20% homologous serum on ice for 15 minutes. Neutrophils at 10⁶ per well were infected with *K. pneumoniae* at a multiplicity of infection of 50 bacteria: 1 neutrophil *in vitro*. Neutrophils were washed with HBSS + gentamicin to remove extracellular or membrane-attached bacteria, lysed with 0.1% Triton-X, and CFU determined at the time points indicated. Data points indicate neutrophils harvested from individual mouse, n=3 mice/group. (D) *In vitro* neutrophil microbial killing assay with cross transfer of WT serum to *thbs1*^{-/-} neutrophils. Conditions are the same as indicated in (C) except *thbs1*^{-/-} neutrophils received bacteria opsonized with either 20% homologous or WT serum. Data points indicate neutrophils harvested from individual mouse, n=3 mice/group. (E) *In vitro* neutrophil microbial killing assay with WT neutrophils receiving either bacteria in WT or *thbs1*^{-/-} serum. Data points indicate neutrophils harvested from individual mouse, n=4 mice/group. Mann-Whitney U rank sum test for 2 group comparisons, Kruskal-Wallis test followed by a Dunn's Multiple Comparisons test for 3 group comparisons, *p<0.05, **p<0.01.

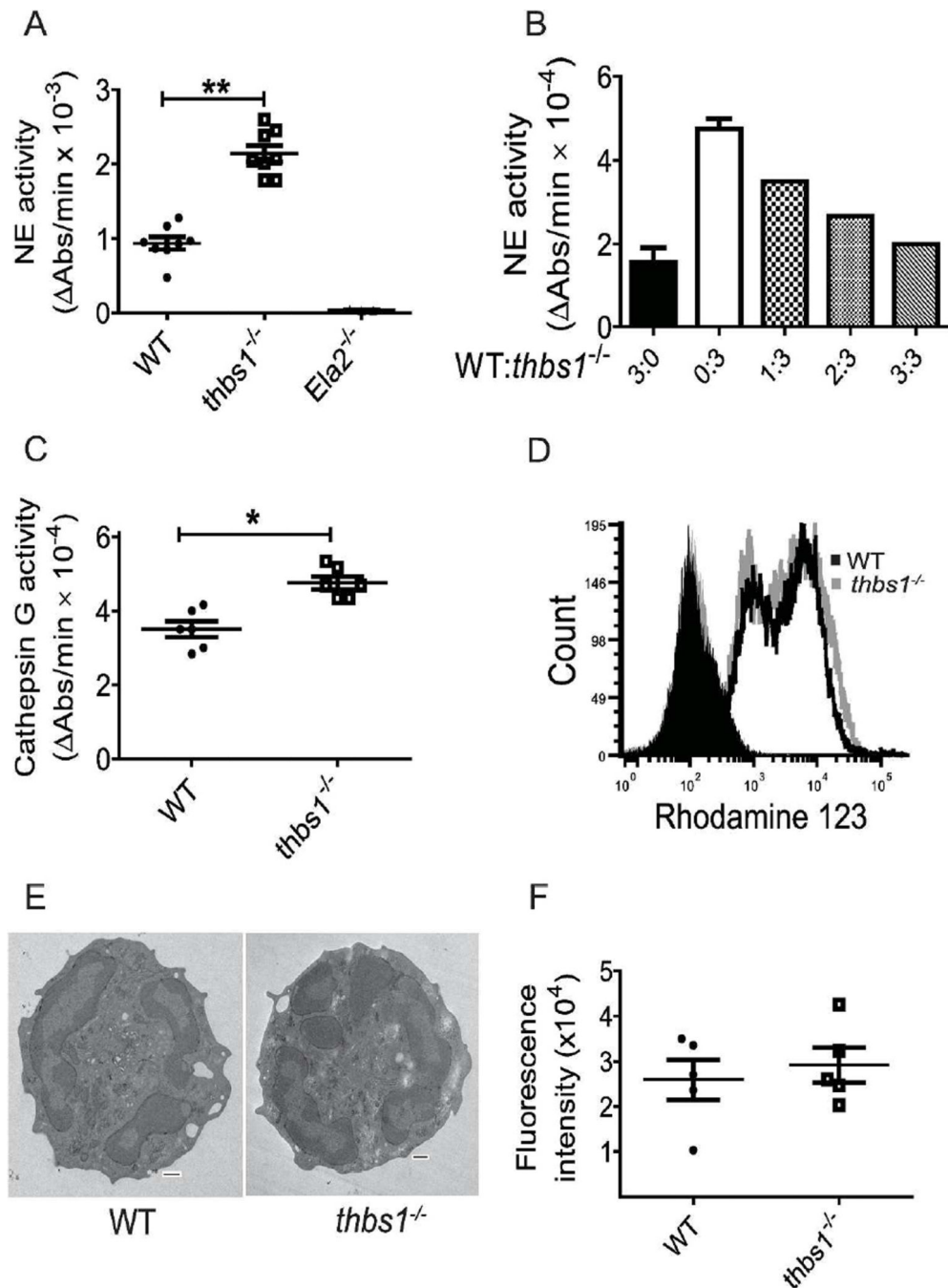


Figure 4. *thbs1*^{-/-} neutrophils show increased NE and CG activity but normal neutrophil oxidative burst, in vitro phagocytosis, and morphology

Neutrophils were harvested from the peritoneum 6 h following 3% thioglycollate injection. (A) NE activity measured as the rate of enzymatic hydrolysis of synthetic NE substrate N-Methoxysuccinyl-Ala-Ala-Pro-Val p-nitroanilide reflected by the increase in Absorbance (Abs) at 405 nm over time utilizing lysates obtained from WT, *thbs1*^{-/-}, and *Ela2*^{-/-} neutrophils. Data points indicate neutrophils obtained from 4 mice/group performed in duplicates. Student's t-test, **p< 0.001. (B) NE activity measured in WT, *thbs1*^{-/-} and

mixtures of WT: *thbs1^{-/-}* neutrophil lysates at differing ratios normalized to protein concentrations. The mixture of neutrophil lysates was generated and pooled from WT and *thbs1^{-/-}* mice at a ratio of 1:3, 2:3, 3:3 where 3 indicates 30 μ L lysate containing 10 μ g protein. Data obtained from WT (3:0, black bar graph) and *thbs1^{-/-}* (0:3, white bar graph) neutrophil lysates. (C) Cathepsin G activity measured as the rate of enzymatic hydrolysis of synthetic CG substrate N-succinyl-Ala-Ala-Pro-Phe-P-nitroanilide reflected by the increase in Absorbance (Abs) at 405 nm over time utilizing lysates obtained from WT, *thbs1^{-/-}* neutrophils. Data points indicate neutrophils obtained from 3 mice/group performed in duplicates. Student's t-test, *p<0.01. (D) Respiratory burst of WT and *thbs1^{-/-}* peritoneal neutrophils as indicated by the shift in fluorescence following oxidation of dihydro-rhodamine [0.4 μ g/mL] to rhodamine. Gray filled histogram: *thbs1^{-/-}* neutrophils at baseline; Black filled histogram: WT neutrophils at baseline; Gray unfilled histogram: *thbs1^{-/-}* neutrophils stimulated with PMA 2 μ g/ml; Black unfilled histogram: WT neutrophils stimulated with PMA 2 μ g/ml. Data obtained from neutrophils pooled from 5 mice/group. (E) Transmission electron microscopy of WT and *thbs1^{-/-}* neutrophils pooled from 5 mice/group. Images are representative of 15 neutrophils examined in each group. Scale bars = 500 nm. (F) In vitro phagocytosis of fluorescence labeled *E. Coli* bioparticles by WT and *thbs1^{-/-}* neutrophils, as indicated by fluorescence intensity. Data points indicate neutrophils obtained from 5 mice/group performed in quadruplicates.

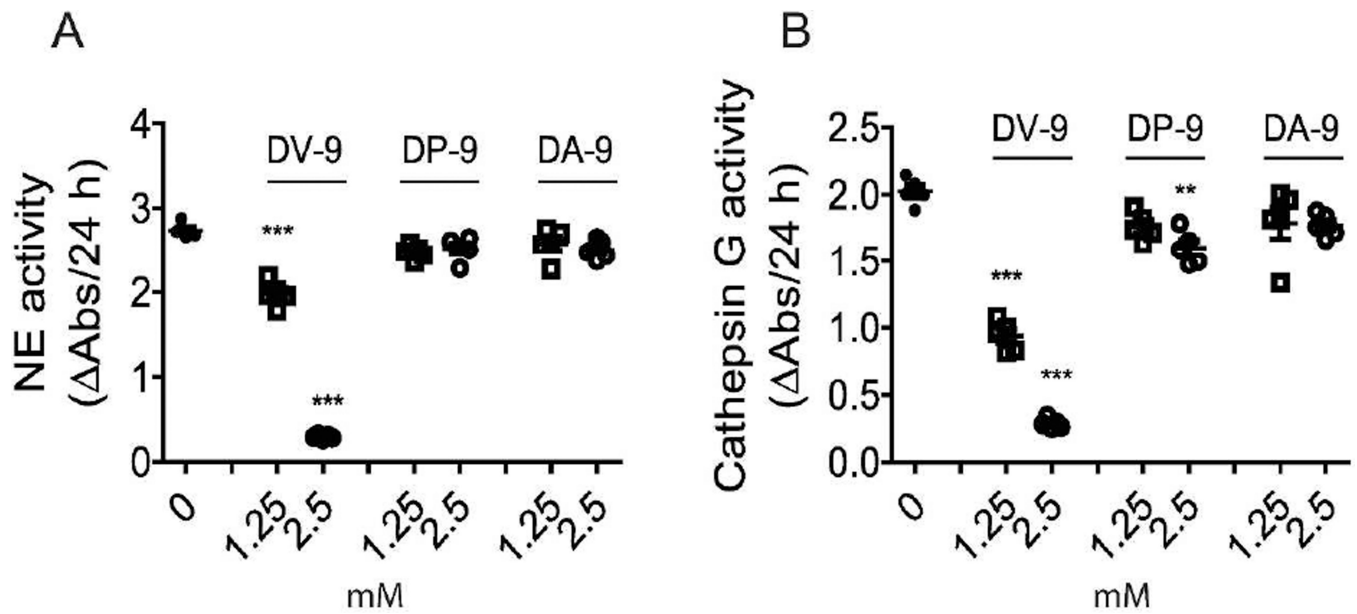


Figure 5. Peptides generated from the thrombospondin-1 type III repeats domain inhibit neutrophil proteolytic function

(A) NE activity measured in WT neutrophil lysates with 1.25 mM or 2.5 mM peptides DV-9 (DNCQYVYNV), DP-9 (DNCPFHYNP), and DA-9 (DNCPYVPNA). Data points indicate neutrophils obtained from 5 mice/group. (B) Cathepsin G activity measured in WT neutrophil lysates 1.25 mM or 2.5 mM peptides DV-9 (DNCQYVYNV), DP-9 (DNCPFHYNP), and DA-9 (DNCPYVPNA). Data points indicate neutrophils obtained from 5 mice/group. ANOVA with Bonferroni multiple comparisons test, ** $p < 0.01$, *** $p < 0.001$.

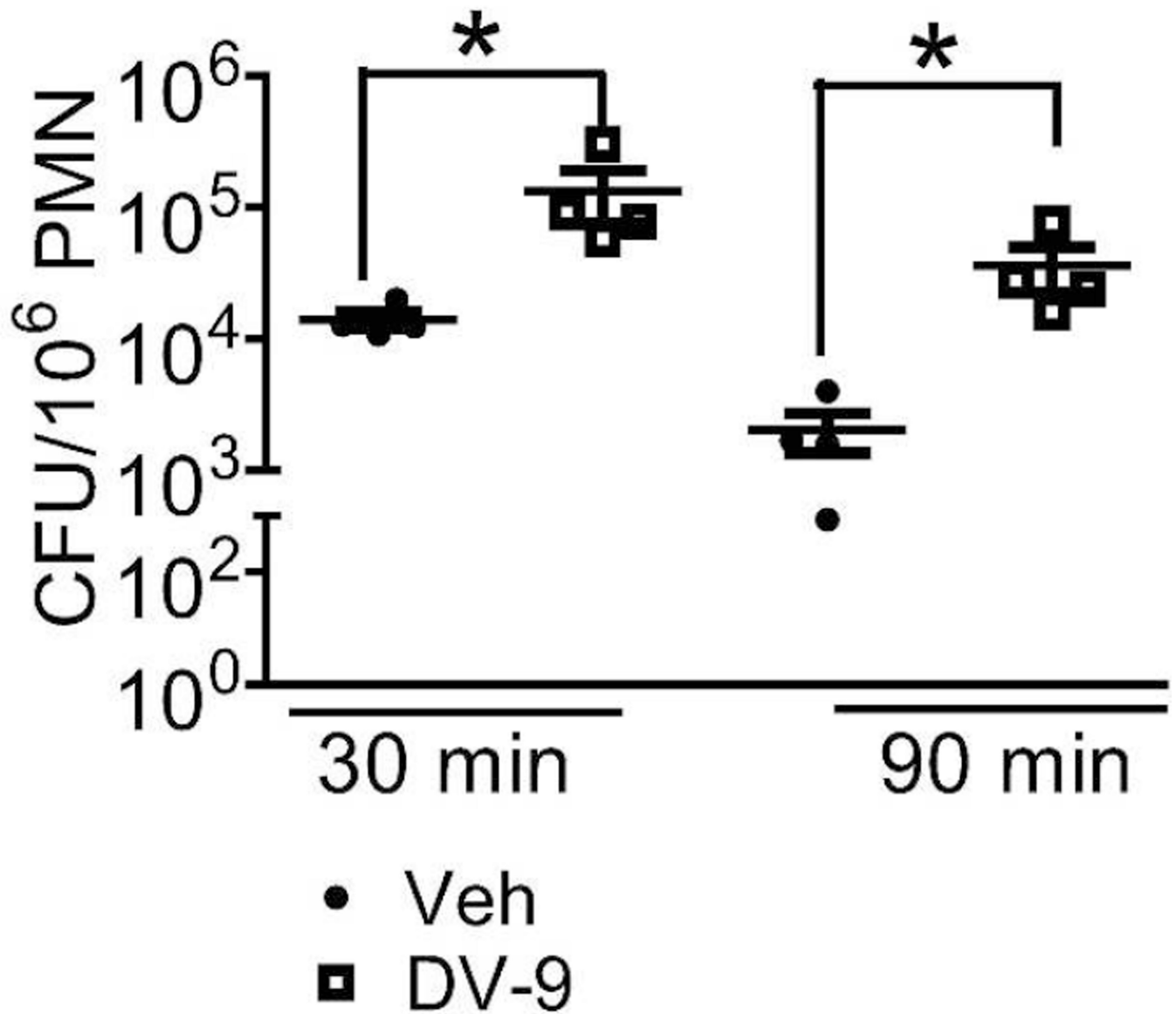


Figure 6. DV-9 peptide impairs neutrophil microbial killing of *K. pneumoniae*
 Intracellular killing by peritoneal neutrophils from WT mice treated with peptide DV-9 or vehicle DMSO just prior to instillation of *K. pneumoniae* in vivo. 30 min represents the initial time point sampled, allowing for neutrophils to engulf bacteria in vivo. Neutrophils were harvested and subsequently plated to quantify CFU at 30 min or incubated further ex vivo for an additional 60 min prior to plating. CFU/10⁶ PMN was obtained for each sample. Data points indicate neutrophils harvested from individual mouse, n=4 mice/group. *p<0.05. Mean-fold reduction in CFU/10⁶ PMN ± SEM over time: Vehicle treatment, 8.3 ± 2.0 compared to DV-9 treatment, 3.5 ± 0.6, Mann-Whitney U test, *p < 0.05.